not elicit any Ca^{2+} response (data not shown). To measure MAP kinase activation, pEF6–*mil*, pEF6–*mil*^{m93} or pEF6–*mil*^{te273} were transiently co-tranfected with a reporter activated by MAP kinase-stimulated Elk-1 (Stratagene) into Jurkat T cells. Normalization of transfection was performed with a pCMV-Renilla luciferase construct and the Stop&Glo reagent (Promega). After stimulation with 100 nM S1P for 4 h, activities of the Firefly and Renilla luciferases were measured in cell lysates. The C305 anti-T-cell receptor antibody gave similar Ca^{2+} and MAP kinase responses in all transfectants.

Phenotypic rescue and genotyping

For RNA injections, the *mil* construct was generated by PCR using wild-type cDNA and cloned into pCS2+. Injected embryos were genotyped using allele-specific restriction fragment length polymorphisms.

Received 17 March; accepted 16 May 2000.

1. Chen, J. N. *et al.* Mutations affecting the cardiovascular system and other internal organs in zebrafish. *Development* **123,** 293–302 (1996).
2. Stainier, D. Y. R. *et al*. Mutations affecting the formation and function of the cardiovascular system in the zebrafish embryo. *Development* **123,** 285–92 (1996).
3. Yelon, D. *et al*. The bHLH transcription factor Hand2 plays parallel roles in zebrafish heart and pectoral fin development. *Development* **127,** 2573–2582 (2000).
4. Yelon, D., Horne, S. & Stainier, D. Y. R. Restricted expression of cardiac myosin genes reveals regulated aspects of heart tube assembly in zebrafish. *Dev. Biol.* **214,** 23–37 (1999).
5. Kikuchi, Y. *et al*. The zebrafish *bonnie and clyde* gene encodes a Mix family homeodomain protein that regulates the generation of endodermal precursors. *Genes Dev.* **14,** 1279–1289 (2000).
6. Reiter, J. F. *et al.* Gata5 is required for the development of the heart and endoderm in zebrafish. *Genes Dev.* **13,** 2983–2995 (1999).
7. Schier, A. F., Neuhauss, S. C., Helde, K. A., Talbot, W. S. & Driever, W. The *one-eyed pinhead* gene functions in mesoderm and endoderm formation in zebrafish and interacts with *no tail*. *Development* **124,** 327–342 (1997).
8. Alexander, J., Rothenberg, M., Henry, G. L. & Stainier, D. Y. R. *casanova* plays an early and essential role in endoderm formation in zebrafish. *Dev. Biol.* **215,** 343–357 (1999).
9. Alexander, J. & Stainier, D. Y. R. *Mutations affecting cardiac development in zebrafish* (eds. Harvey, R. & Rosenthal, N.) (Academic, San Diego, 1999).
10. Strähle, U., Blader, P., Henrique, D. & Ingham, P. W. *axial*, a zebrafish gene expressed along the developing body axis, shows altered expression in *cyclops* mutant embryos. *Genes Dev.* **7,** 1436–1446 (1993).
11. Knapik, E. W. *et al.* A microsatellite genetic linkage map for zebrafish (Danio rerio). *Nature Genet.* **18,** 338–343 (1998).
12. Chan, F. Y. *et al.* Characterization of adult alpha- and beta-globin genes in the zebrafish. *Blood* **89,** 688–700 (1997).
13. Martin, C. C., Laforest, L., Akimenko, M. A. & Ekker, M. A role for DNA methylation in gastrulation and somite patterning. *Dev. Biol.* **206,** 189–205 (1999).
14. Okazaki, H. *et al.* Molecular cloning of a novel putative G protein-coupled receptor expressed in the cardiovascular system. *Biochem. Biophys. Res. Commun.* **190,** 1104–1109 (1993).
15. An, S. *et al.* Identification of cDNAs encoding two G protein-coupled receptors for lysosphingolipids. *FEBS Lett.* **417,** 279–282 (1997).
16. MacLennan, A. J., Browe, C. S., Gaskin, A. A., Lado, D. C. & Shaw, G. Cloning and characterization of a putative G-protein coupled receptor potentially involved in development. *Mol. Cell. Neurosci.* **5,** 201–209 (1994).
17. An, S., Bleu, T. & Zheng, Y. Transduction of intracellular calcium signals through G protein-mediated activation of phospholipase C by recombinant sphingosine 1-phosphate receptors. *Mol. Pharmacol.* **55,** 787–794 (1999).
18. Goetzl, E. J. & An, S. Diversity of cellular receptors and functions for the lysophospholipid growth factors lysophosphatidic acid and sphingosine 1-phosphate. *FASEB J.* **12,** 1589–1598 (1998).
19. An, S., Zheng, Y. & Bleu, T. Sphingosine 1-phosphate-induced cell proliferation, survival, and related signaling events mediated by G protein-coupled receptors Edg3 and Edg5. *J. Biol. Chem.* **275,** 288–296 (2000).
20. Lee, M. J. *et al.* Sphingosine-1-phosphate as a ligand for the G protein-coupled receptor EDG-1. *Science* **279,** 1552–1555 (1998).
21. Forbes, A. & Lehmann, R. Cell migration in *Drosophila*. *Curr. Opin. Genet. Dev.* **9,** 473–478 (1999).
22. Zhang, N., Zhang, J., Purcell, K. J., Cheng, Y. & Howard, K. The *Drosophila* protein Wunen repels migrating germ cells. *Nature* **385,** 64–67 (1997).
23. Roberts, R., Sciorra, V. A. & Morris, A. J. Human type 2 phosphatidic acid phosphohydrolases. Substrate specificity of the type 2a, 2b, and 2c enzymes and cell surface activity of the 2a isoform. *J. Biol. Chem.* **273,** 22059–22067 (1998).
24. Scheer, A. *et al.* Mutational analysis of the highly conserved arginine within the glu/asp-arg-tyr motif of the α_{1b}-adrenergic receptor: effects on receptor isomerization and activation. *Mol. Pharmacol.* **57,** 219—231 (2000).
25. Strader, C. D., Fong, T. M., Tota, M. R., Underwood, D. & Dixon, R. A. Structure and function of G protein-coupled receptors. *Annu. Rev. Biochem.* **63,** 101–132 (1994).
26. Hla, T. *et al.* Sphingosine-1-phosphate: extracellular mediator or intracellular second messenger? *Biochem. Pharmacol.* **58,** 201–207 (1999).
27. Spiegel, S. Sphingosine 1-phosphate: a prototype of a new class of second messengers. *J. Leukocyte Biol.* **65,** 341–344 (1999).
28. Moolenaar, W. H. Bioactive lysophospholipids and their G protein-coupled receptors. *Exp. Cell Res.* **253,** 230–238 (1999).

Supplementary information is available on *Nature*'s World-Wide Web site (http://www.nature.com) or as paper copy from the London editorial office of *Nature*.

Acknowledgements

We thank I. Herskowitz, H. Bourne, C. Bargmann, R. Lehmann and members of the lab for discussions and comments on the manuscript. We are also grateful to A. Navarro for excellent fish care. E.K. is supported by the University of California President's post-doctoral fellowship program. This work was supported in part by the Program in Human Genetics Genomics Core Facility at UCSF as well as by grants to D.Y.R.S. from the American Heart Association and the Packard Foundation.

Correspondence and requests for materials should be addressed to D.Y.R.S. (e-mail: didier_stainier@biochem.ucsf.edu). The cDNA sequence of *mil* has been deposited in GenBank under accession number AF260256.

A one-hit model of cell death in inherited neuronal degenerations

Geoff Clarke*†, Richard A. Collins†, Blair R. Leavitt‡, David F. Andrews§, Michael R. Hayden‡, Charles J. Lumsden‖ & Roderick R. McInnes*†‖¶

** Programs in Developmental Biology and Genetics, The Research Institute, Hospital for Sick Children, 555 University Ave., Toronto, Ontario M5G 1X8, Canada*

† Departments of Molecular and Medical Genetics, ¶ Pediatrics, and ‖ Department of Medicine, Institute of Medical Science, University of Toronto, 1 King's College Circle, Toronto, Ontario M5S 1A8, Canada

‡ Centre for Molecular Medicine and Therapeutics, Department of Medical Genetics University of British Columbia, Vancouver, British Columbia V5Z 4H4, Canada

§ Department of Statistics, University of Toronto, 100 St. George Street, M5S 3G3, Canada

In genetic disorders associated with premature neuronal death, symptoms may not appear for years or decades. This delay in clinical onset is often assumed to reflect the occurrence of age-dependent cumulative damage[1–6]. For example, it has been suggested that oxidative stress disrupts metabolism in neurological degenerative disorders by the cumulative damage of essential macromolecules[1,4,7]. A prediction of the cumulative damage hypothesis is that the probability of cell death will increase over time. Here we show in contrast that the kinetics of neuronal death in 12 models of photoreceptor degeneration, hippocampal neurons undergoing excitotoxic cell death[8], a mouse model of cerebellar degeneration[9] and Parkinson's[10] and Huntington's diseases are all exponential and better explained by mathematical models in which the risk of cell death remains constant or decreases exponentially with age. These kinetics argue against the cumulative damage hypothesis; instead, the time of death of any neuron is random. Our findings are most simply accommodated by a 'one-hit' biochemical model in which mutation imposes a mutant steady state on the neuron and a single event randomly initiates cell death. This model appears to be common to many forms of neurodegeneration and has implications for therapeutic strategies.

To distinguish between the increasing risk of death associated with cumulative damage (which would generate a sigmoidal decline in cell number) and the exponential decline in cell number that results from a constant or decreasing risk of death (Fig. 1a), we used regression analysis to analyse photoreceptor neuron death in 11 animal models of inherited retinal degeneration and an experimental model of retinal detachment. These models include animals with mutations in genes encoding a range of proteins including the photosensitive pigment rhodopsin (M. M. LaVail, personal communication), the enzyme cyclic GMP phosphodiesterase[11,12] and the structural proteins rom-1 (ref. 13) and peripherin/rds[14,15]. In three other mutants analysed, the affected gene is unknown.

In five of these examples (Fig. 1, Table 1, and see Supplementary Information), the data fit only to mathematical models in which the probability of photoreceptor death remains constant with age. In six

others (Fig. 2, Table 1), the kinetics fit equally well to models of constant or exponentially decreasing risk of death. Consequently, in all of these animal models the increasing risk of photoreceptor death predicted by the cumulative damage hypothesis can be excluded, a possible exception being the $Rd^{-/-}$ mouse in which the data (Fig. 1d) fit equally well to models of constant ($R^2 = 0.985$, $P < 0.001$) and exponentially increasing risk ($R^2 = 0.980$; $P < 0.001$). Thus, even if age-dependent cumulative damage does occur in these mutant retinas, it is not associated with an increase in the probability that the photoreceptors will die.

In agreement with these direct measurements of the kinetics of photoreceptor death in animal models, clinical assessment of photoreceptor function in patients with retinitis pigmentosa and cone-rod dystrophy has shown that both visual field loss[16] and the decay of the maximum photoreceptor electroretinogram responses also observe exponential kinetics[17,18]. Thus, the exponential cell death kinetics that we have identified in animal models appear to be shared by most, if not all, examples of inherited retinal degeneration.

To determine whether a constant or exponentially decreasing risk of neuronal death is a general phenomenon shared by other classes of neuron, we examined the kinetics of neurodegeneration in four other diseases or experimental models. Neuronal loss in the substantia nigra in Parkinson's disease[10], the excitotoxic death of cultured hippocampal neurons[8] and the loss of cerebellar granule cells in *pcd/pcd* (Purkinje cell degeneration) mice[9] have been shown to produce an exponential decline in neuronal number with time. Our regression analyses demonstrate that only a constant risk describes the kinetics of cell death in the first two of these examples (Table 1, Fig. 3a, b). On the other hand, the loss of cerebellar granule cells subsequent to the genetically determined loss of their target Purkinje neurons in *pcd/pcd* mice[9] (Fig. 3c) and neuronal death in a

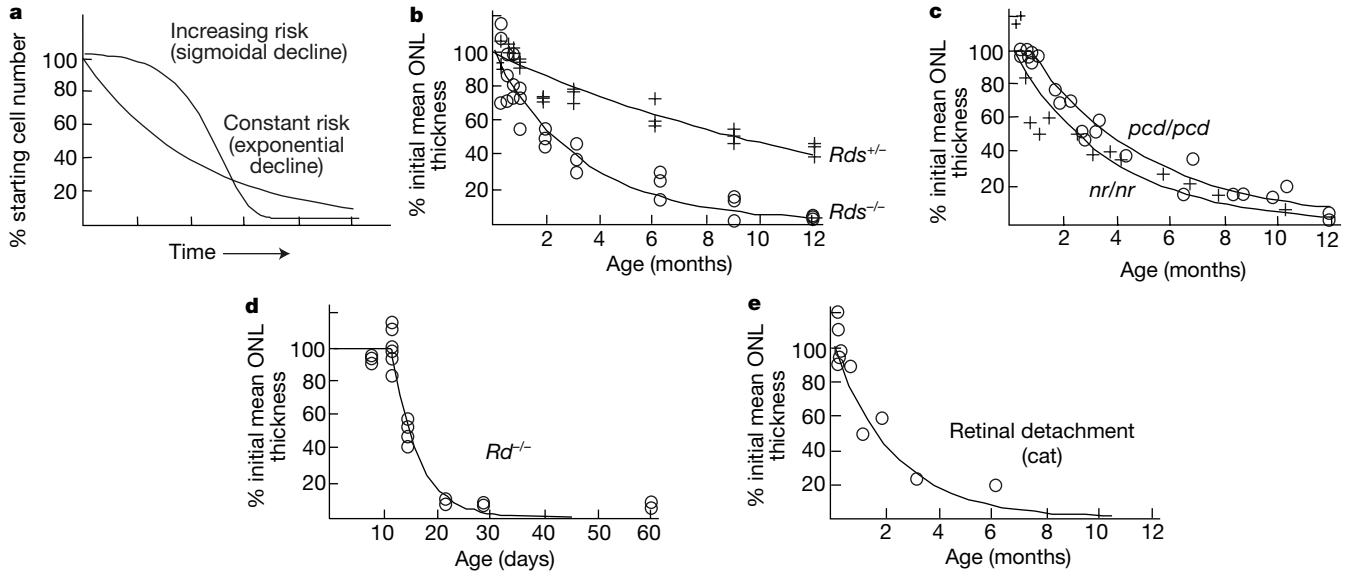

Figure 1 Animal models of inherited photoreceptor degeneration and retinal detachment, in which the kinetics of cell death are best described by a constant risk of neuronal death (see equations (1) and (3) in Methods). **a**, Constant and increasing risk of neuronal death will manifest as an exponential or sigmoidal decline in cell number, respectively. **b**, *Retinal degeneration slow* heterozygous ($Rds^{+/-}$)[15] and homozygous mice ($Rds^{-/-}$)[15] carrying a null mutation in the gene encoding peripherin/rds. **c**, *Nervous* homozygous mice (*nr/nr*)[27], and *purkinje cell degeneration* mice (*pcd/pcd*)[28]. **d**, Mice homozygous for a null mutation in the gene encoding the phototransduction enzyme rod cGMP β-phosphodiesterase ($Rd^{-/-}$)[14]. **e**, Experimental retinal detachment in the cat[24].

Table 1 Parameter estimates for kinetic models relating the risk of neuronal death (μ) to age

Animal model	Constant μ: $\frac{d\mathrm{ONL}(t)}{dt} = -\mu \times \mathrm{ONL}(t)$			Exponentially decreasing μ: $\frac{d\mathrm{ONL}(t)}{dt} = -\mu_0 e^{-At} \times \mathrm{ONL}(t)$			
	μ	ONL(0)	R^{2*}	μ_0	A	ONL(0)	R^{2*}
$Rds^{+/-}$ mice[15]	0.0170	49.4 μm	0.992	N/A	N/A	N/A	rejected†
$Rds^{-/-}$ mice[15]	0.0729	40.5 μm	0.968	N/A	N/A	N/A	rejected†
nr/nr mice‡[27]	0.278	50.1 μm	0.953	N/A	N/A	N/A	rejected†
Photoreceptors of *pcd/pcd* mice[28]	0.223	10.6 nuclei	0.992	N/A	N/A	N/A	rejected†
Retinal detachment (cat)‡[24]	0.00752	220 nuclei per mm	0.976	N/A	N/A	N/A	rejected†
$Rom1^{-/-}$ mice[13]	0.0316	37.7 μm	0.993	0.0666	0.103	41.9 μm	0.995
pd (miniature schnauzer)[12]	2.24	12.1 nuclei	0.979	3.13	1.12	13.1 nuclei	0.992
Albino (Balb/cHeA) mice[14]	0.00917	51.7 μm	0.995	0.0235	0.0485	51.7 μm	0.997
rcd-1 (Irish setter)[11,12]	0.0289	10.6 nuclei	0.957	0.0483	0.086	11.8 nuclei	0.970
$Rd^{-/-}$;$Rds^{-/-}$ mice[14]	0.123	45.4 μm	0.992	0.208	0.0912	45.3 μm	0.996
P23H rhodopsin-expressing transgenic rat§	0.0095	46.8 μm	0.975	0.0172	0.00752	55.0 μm	0.987
$Rd^{-/-}$ mice[14]	0.208	42.2 μm	0.985	N/A	N/A	N/A	rejected†
Cultured hippocampal neurons[8]	0.0773	100% of normal	0.996	N/A	N/A	N/A	rejected†
Parkinson's disease[10]	0.0858	100% of normal	0.919	N/A	N/A	N/A	rejected†
Granule cell degeneration in *pcd/pcd* mice[9]	0.006	5,999.52 cells	0.990	0.0076	0.0018	6,000 cells	0.990
Chemically-induced rat model of Parkinson's disease[19]‡	0.207	100% of normal	0.967	0.537	0.310	100%	0.999

* R^2 values reflect the proportion of data variability that is explained by the model. All reported R^2 values were statistically significant ($P < 0.001$).
† Parameter estimates were not significantly different from zero.
‡ Regressions performed on mean values reported in literature.
N/A, not applicable.
§ M. M. LaVail, personal communication.

chemically induced rat model of Parkinson's disease[19] (Fig. 3d) can both be described by either a constant or an exponentially decreasing risk of cell death (Table 1). We also measured ^{18}F-doxyglucose uptake in the caudate nuclei of patients with Huntington's disease as an indirect measure of neuronal loss. Because each of these patients was repeatedly tested at various times after clinical onset, the glucose uptake data, predictably, is highly variable in the whole population of patients (see Supplementary Information). Consequently, analysis of neuronal degeneration kinetics in this heterogeneous population necessitated the use of repeated-measures regression for each individual (see Methods). We found that neurodegeneration in these patients is also best described by a constant risk of cell death (Fig. 3e). Thus, our identification of similar cell death kinetics in five different types of neuron indicates that a constant or decreasing risk of cell death may be common to many forms of neurodegeneration. Although neuronal death is mediated by apoptosis in all photoreceptor degenerations examined (for example, refs 7, 20), it remains to be determined whether a constant or exponentially decreasing risk of death will be found invariably to accompany neuronal apoptosis.

Although the available data do not allow us to distinguish conclusively between constant and exponentially decreasing risk, both models indicate that the time of death of an individual neuron is random. Nevertheless, the two models have quite different pathophysiological implications. In a process involving constant risk, the time of death of an individual neuron is not only random, but also independent of the time of death of any other neuron. In this case, the kinetics of neuronal degeneration are comparable to the simple exponential decay exhibited by radioactive compounds, and the different rates of photoreceptor degeneration (Fig. 1) are determined largely or solely by the mutant genotype. In contrast, exponentially decreasing risk indicates that the chance of cell death decreases in direct proportion to the number of remaining cells. Such kinetics could result from an increase in the concentration of a

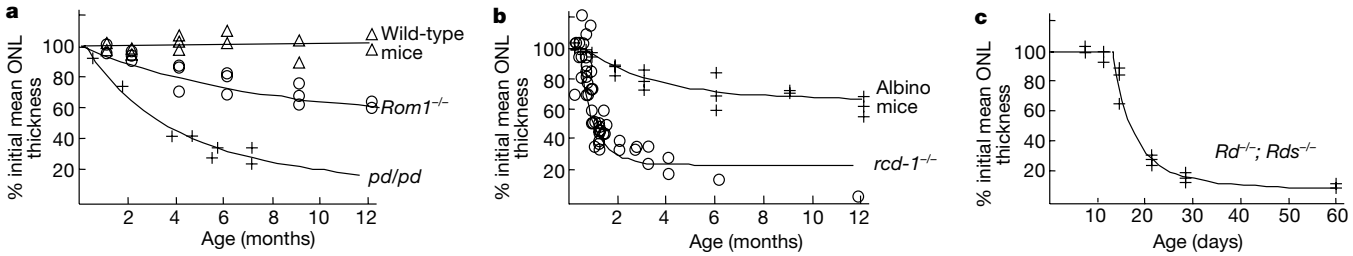

Figure 2 Animal models of inherited photoreceptor degeneration in which the kinetics of cell death are best described by an exponentially decreasing risk of death (see equations 1 and 2 in Methods). **a**, Wild-type and *Rom1*$^{-/-}$ mice[13], and photoreceptor dysplasia (*pd/pd*) in miniature schnauzers[12]. **b**, Albino mice[14] (Balb/cHeA) and rod-cell degeneration (*rcd-1*) in Irish setters[11,12] due to a null mutation in the rod cGMP β-phosphodiesterase gene. **c**, Mice homozygous for null mutations in both the gene encoding rod cGMP β-phosphodiesterase and the gene encoding peripherin/rds (*Rd*$^{-/-}$;*Rds*$^{-/-}$)[14].

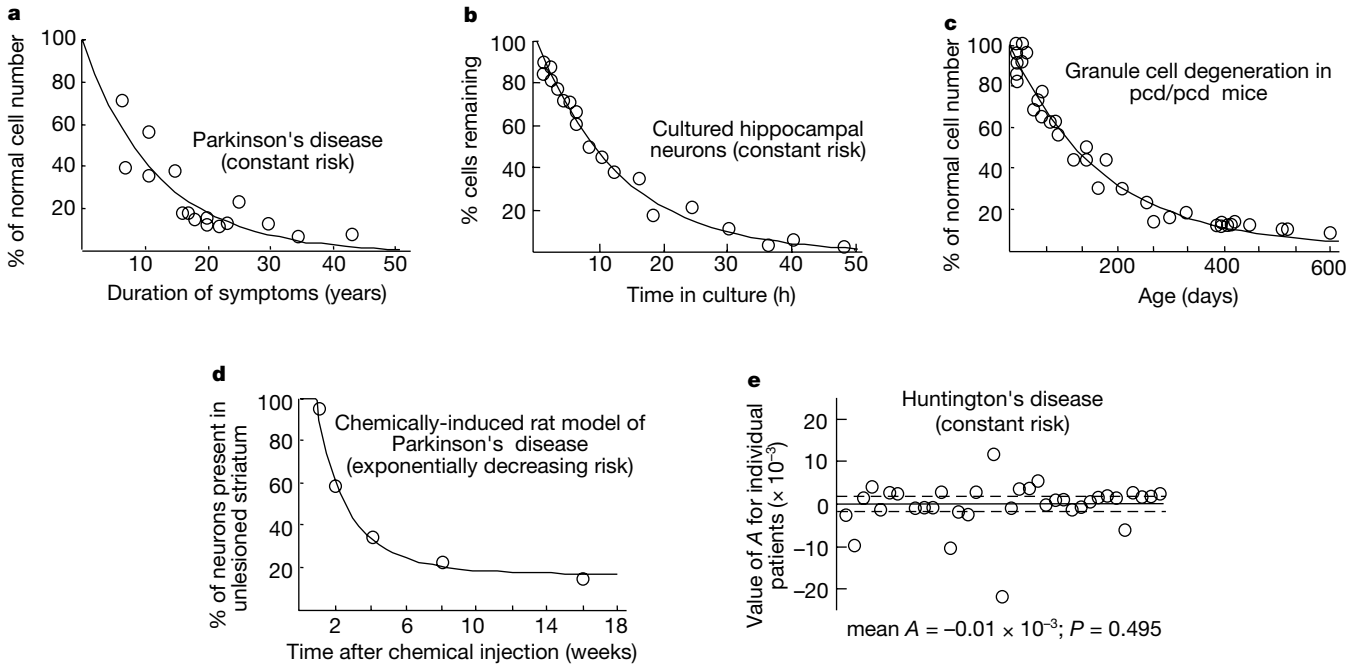

Figure 3 Examples of non-retinal neuronal death that display a constant or exponentially decreasing risk of death. **a**, The number of neurons (% of normal) in the substantia nigra of patients with Parkinson's disease as a function of symptom duration[10] is best described by a constant probability of neuronal death. **b**, Cultured hippocampal neurons undergoing excitotoxic cell death after incubation with glutamate exhibit a constant risk of cell death[8]. **c**, In contrast, the secondary loss of cerebellar granule cells[9] is described equally well by either a constant or an exponentially decreasing risk of cell death; the curve represents a constant risk. **d**, The percentage of substantia nigra neurons present in rats after injection with the neurotoxin 6-hydroxydopamine[19], a chemically induced animal model of Parkinson's disease, is best fit by an exponentially decreasing risk of neuronal death. **e**, The kinetics of metabolic decline in Huntington's disease patients are best fit by a constant risk of cell loss. Values of A (in the exponent of equation (5), see Methods) do not differ significantly from zero (P = 0.495, Student's t-test). Each point represents the estimated A for an individual patient. Solid line, mean A (mean ± s.d.: $-0.01 \times 10^{-3} \pm 5.3 \times 10^{-3}$ mM h^{-1}, n = 38 patients) across patient population; dashed lines, 95% confidence interval for the mean value of A (-1.7×10^{-3}, 1.7×10^{-3}).

survival factor, such as basic fibroblast growth factor or ciliary neurotrophic factor[21], or from a decrease in the amount of a toxic factor as the population of cells declines. Consistent with the latter possibility, dying retinal progenitor cells have been shown to produce an apoptosis-inducing agent[22].

An alternative interpretation for the exponential decline in risk is that the decrease is an artefact resulting from the presence of two neuronal populations, each with different but constant risks of cell death. For photoreceptor degenerations, this possibility is excluded by the fact that 97% of mouse photoreceptors are rods and only 3% are cones[23]. This proportion of cones is too small to influence the overall kinetics of photoreceptor death. Furthermore, the data for all six models exhibiting a decreasing risk do not fit a simple equation incorporating two exponential functions (see Supplementary Information), which also suggests that the presence of two differentially affected cell populations is not responsible for the exponentially decreasing risk of cell death.

Any model of the mechanisms underlying inherited neuronal degenerations must account for the major features of cell death in these disorders. These features are (1) the constant or decreasing risk of neuronal death described above; (2) the genotype-dependent nature of the risk; (3) the random time of death of any cell (illustrated by the random distribution of apoptotic photoreceptors seen in the retinas of animals and humans with inherited retinal degenerations[13,20]); and (4) the paradoxical situation in which most neurons in animals or patients with inherited neurodegenerations survive and function normally for months, years or decades, while a few genetically identical cells in the population are dying randomly.

We propose that these features can be explained if the mutant neurons are in an abnormal homeostatic state, the mutant steady state (MSS). The MSS differs little from the normal neuronal steady state (as most of the mutant cells are alive and functioning normally), except that the MSS is associated with an increased risk of cell death. We suggest that the MSS is a response to mutation characterized by subtle but critical changes in the expression or function of relatively few 'mutant response' genes or proteins (MuRGs or MuRPs, respectively), which mediate critical pre-death reactions. If MuRP is an enzyme, for example, it may change the relative concentrations of 'pre-lethal' molecules (Fig. 4). Exit from the MSS and commitment to cell death would occur when random fluctuations in the concentrations of pre-lethal molecules exceed a threshold beyond which neuronal death is initiated. Different mutations would shift the steady state to varying degrees, so that mutations producing a transition to an MSS closer to the cell-death threshold have a greater chance of exceeding that threshold, and therefore a higher probability of causing cell death. Thus, we propose a 'one-hit' model in which the death of an individual neuron is initiated randomly in time by a single rare catastrophic event.

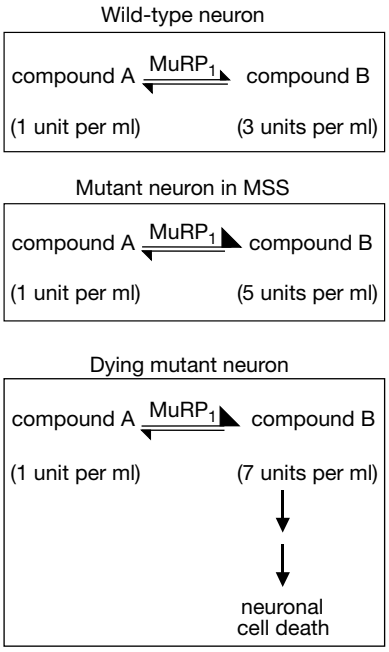

Figure 4 The exponential kinetics of cell death in inherited neuronal degenerations suggest the existence of a mutant steady state (MSS) in which the risk of cell death is increased. In wild-type neurons, a reaction, catalysed for example by the enzyme $MuRP_1$, is associated with a concentration of compound B of 3 units per ml. In a mutant neuron in the MSS, the $MuRP_1$ activity changes in response to the mutation, so that the concentration of compound B is increased to 5 units per ml. Random increases in the concentration of compound B to 7 units per ml will trigger cell death.

A similar one-hit kinetic model has been proposed and rejected as an explanation for the exponential cell death kinetics exhibited by cultured hippocampal neurons exposed transiently to excitotoxic amino acids[8]. The one-hit model was rejected in favour of a more complex mechanism involving a multistep biochemical cascade in which the overall death rate is determined by the specific rate constants for each of an unknown number of transitions within the cascade. We suggest, however, that some environmental insults place neurons in an abnormal steady state which, like the MSS, is associated with a constant increased risk of death. This environmentally induced abnormal steady state is exemplified by the effect of excitotoxic amino acids in initiating the exponential death of hippocampal neurons[8] (Fig. 3b, Table 1) and by the effect of retinal detachment in leading to photoreceptor death[24] (Fig. 1e, Table 1).

Our findings have important implications for the understanding and treatment of retinal and possibly other types of neuronal degeneration. First, biochemical mechanisms proposed to underlie neuronal death must be re-examined in light of the constant or exponentially decreasing risk of cell death that we have identified. Second, identification of the MuRGs and MuRPs in different mutant neurons will indicate whether mutations impose MSSs that share common MuRGs and MuRPs, or whether each MSS is uniquely or partly defined by the specific mutant gene or mutation. In mutant neurons in which the risk of death is constant throughout life, the MSS should be the same in young and old cells with the same genotype, although additional secondary changes in gene or protein expression may occur as a consequence of cell death. Alternatively, in models in which the risk of death decreases exponentially, cell death may be associated with a changing pattern of MuRGs and MuRPs. In either case, identification of MuRGs and MuRPs in different mutants is likely to provide insight into the pathogenic events that increase the risk of cell death in the MSS. Pharmacological intervention to shift the activity of MuRGs and MuRPs towards normal levels should slow or prevent initiation of the biochemical cascade leading to cell death. Finally, the absence of cumulative damage means that the likelihood that a mutant neuron can be rescued by treatment is not diminished by age, although fewer cells will be available to rescue. Therefore, treatment at any stage of the illness is likely to confer benefit. □

Methods

Measurements and statistical analysis

We examined the kinetics of photoreceptor degeneration in animal models in which cell loss had been reported quantitatively over at least one year, or until most photoreceptors had died. The kinetics of cell loss were analysed by fitting either the outer nuclear layer (ONL) thickness or cell number data to solutions of the differential equation

$$\frac{d\mathrm{ONL}(t)}{dt} = -\mu(t) \times \mathrm{ONL}(t) \quad (1)$$

where $\mu(t)$ represents the risk of cell death at age t. Functions for $\mu(t)$ were substituted as

follows:

$$\text{exponentially decreasing risk} \quad \mu(t) = \mu_0 e^{-A(t-\text{delay})} \tag{2}$$

$$\text{constant risk} \quad \mu(t) = \mu_0 \tag{3}$$

$$\text{exponentially increasing risk} \quad \mu(t) = \mu_0 e^{A(t-\text{delay})} \tag{4}$$

where μ_0 represents the initial probability of cell death and delay represents the time before neuronal death begins. Equations for $\mu(t)$ were chosen on the basis of their ability to yield exponential and sigmoidal curves. Data fitting was performed using nonlinear regression analysis (quasi-Newton methods), a method of modelling the relationship between variables, using the functions in the Mathematica 3.0 (Wolfram Research) software package[25]. Models were rejected if parameter estimates did not differ significantly ($P < 0.05$) from zero.

Measurements of metabolic decline in the caudates of 38 patients with Huntington's disease were obtained from PET scans as described[26]. For each patient, average glucose uptake over the course of at least three years was fit to the solution of the differential equation:

$$\frac{d\text{ONL}(t)}{dt} = \mu e^{At} \times \text{ONL}(t) \tag{5}$$

to provide an estimate of A. $A > 0$ corresponds to increasing risk, $A < 0$ to decreasing risk, and $A = 0$ to constant risk. Estimates of A for each subject were then averaged, and a Student's t-test was used to determine whether the mean value was significantly different from zero ($P < 0.05$).

Received 15 February; accepted 22 May 2000.

1. Coyle, J. T. & Puttfarken, P. Oxidative stress, glutamate, and neurodegenerative disorders. *Science* **262,** 689–695 (1993).
2. Cummings, J. L., Vinters, H. V., Cole, G. M. & Khachaturian, Z. S. Alzheimer's disease: etiologies, pathophysiology, cognitive reserve, and treatment opportunities. *Neurology* **51,** S2–17 (1998).
3. Alves-Rodrigues, A., Gregori, L. & Figueiredo-Pereira, M. E. Ubiquitin, cellular inclusions and their role in neurodegeneration. *Trends Neurosci.* **21,** 516–520 (1998).
4. Cassarino, D. S. & Bennett, J. P. Jr An evaluation of the role of mitochondria in neurodegenerative diseases: mitochondrial mutations and oxidative pathology, protective nuclear responses, and cell death in neurodegeneration. *Brain Res. Rev.* **29,** 1–25 (1999).
5. Selkoe, D. J. Translating cell biology into therapeutic advances in Alzheimer's disease. *Nature* **399,** A23–A31 (1999).
6. Dunnett, S. B. & Björklund, A. Prospects for new restorative and neuroprotective treatments in Parkinson's disease. *Nature* **399,** A32–A39 (1999).
7. Travis, G. H. Mechanisms of cell death in the inherited retinal degenerations. *Am. J. Hum. Genet.* **62,** 503–508 (1998).
8. Dubinsky, J. M., Kristal, B. S. & Elizondo-Fournier, M. On the probabilisitic nature of excitotoxic neuronal death in hippocampal neurons. *Neuropharmacology* **34,** 701–711 (1995).
9. Triarhou, L. C. Rate of neuronal fallout in a transsynaptic cerebellar model. *Brain Res. Bull.* **47,** 219–222 (1998).
10. Fearnley, J. M. & Lees, A. J. Ageing and Parkinson's disease: substantia nigra regional selectivity. *Brain* **114,** 2283–2301 (1991).
11. Schmidt, S. Y. & Aguirre, G. D. Reductions in taurine secondary to photoreceptor loss in Irish setters with rod-cone dysplasia. *Invest. Ophthalmol. Vis. Sci.* **26,** 679–683 (1985).
12. Parshall, C. J., Wyman, M., Nitroy, S., Acland, G. & Aguirre, G. Photoreceptor dysplasia: an inherited progressive retinal atrophy of miniature schnauzer dogs. *Prog. Vet. Comp. Ophthalmol.* **1,** 187–203 (1991).
13. Clarke, G. *et al.* Rom-1 is required for rod photoreceptor viability and the regulation of disk morphogenesis. *Nature Genet.* **25,** 67–73 (2000).
14. Sanyal, S. & Hawkins, R. K. Genetic interaction in the retinal degeneration of mice. *Exp. Eye Res.* **33,** 213–222 (1981).
15. Hawkins, R. K., Jansen, H. G. & Sanyal, S. Development and degeneration of retina in *rds* mutant mice: photoreceptor abnormalities in the heterozygotes. *Exp. Eye Res.* **41,** 701–720 (1985).
16. Massof, R. W., Dagnelie, G., Benzschawel, T., Palmer, R. W. & Finkelstein, D. First order dynamics of visual field loss in retinitis pigmentosa. *Clin. Vis. Sci.* **5,** 1–26 (1990).
17. Berson, E. L., Sandberg, M. A., Rosner, B., Birch, D. G. & Hanson, A. H. Natural course of retinitis pigmentosa over a three-year interval. *Am. J. Ophthalmol.* **99,** 240–251 (1985).
18. Birch, D. G., Anderson, J. L. & Fish, G. E. Yearly rates of rod and cone functional loss in retinitis pigmentosa and cone-rod dystrophy. *Ophthalmology* **106,** 258–268 (1999).
19. Sauer, H. & Oertel, W. H. Progressive degeneration of nigrostriatal dopamine neurons following intrastriatal terminal lesions with 6-hydroxydopamine: a combined retrograde tracing and immunocytochemical study in the rat. *Neuroscience* **59,** 401–415 (1994).
20. Li, Z.-Y. & Milam, A. H. in *Degenerative Diseases of the Retina* (eds Anderson, R. E., LaVail, M. M. & Hollyfield, J. G.) 1–8 (Plennum, New York, 1995).
21. Wen, R. *et al.* Injury-induced upregulation of bFGF and CNTF mRNAs in the rat retina. *J. Neurosci.* **15,** 7377–7385 (1995).
22. Seigal, G. S. & Liu, L. Inducible, apoptosis-promoting activity in retinal cell-conditioned medium. *Mol. Vision* **3,** 14 (1997).
23. Carter-Dawson, L. D. & LaVail, M. M. Rods and cones in the mouse retina. I. Structural analysis using light and electron microscopy. *J. Comp. Neurol.* **188,** 245–262 (1979).
24. Erickson, P. A., Fisher, S. K., Anderson, D. H., Stern, W. H. & Borgula, G. A. Retinal detachment in the cat: the outer nuclear and outer plexiform layers. *Invest. Ophthalmol. Vis. Sci.* **24,** 927–942 (1983).
25. Ratkowsky, D. A. *Nonlinear Regression Modeling: A Unified Practical Approach* (Marcel Decker, New York, 1983).
26. Kremer, B. *et al.* Influence of lamotrigine on progression of early Huntington's disease: a randomized clinical trial. *Neurology* **53,** 1000–1011 (1999).
27. La Vail, M. M. *et al.* Retinal degeneration in the nervous mouse. I. Light microscopic cytopathology and changes in the interphotoreceptor matrix *J. Comp. Neurol.* **333,** 168–181 (1993).
28. LaVail, M. M., Blanks, J. C. & Mullen, R. J. Retinal degeneration in the pcd cerebellar mouse. I. Light microscopic and autoradiographic analysis. *J. Comp. Neurol.* **212,** 217–230 (1982).

Supplementary information is available on *Nature*'s World-Wide Web site (http://www.nature.com) or as paper copy from the London editorial office of *Nature*.

Acknowledgements

We thank the physicians of the Huntington's disease patients for their help and support of this study; M. LaVail for sharing unpublished data on P23H rhodopsin-expressing transgenic rats; and A. G. Kundson Jr, T. P. Dryja, D. J. Zack, H. Lipshitz, M. W. Salter and S. Meyn for critical reading of the manuscript. This work was supported by grants from the Foundation Fighting Blindness (R.R.M.), The Macular Vision Research Foundation (R.R.M.), The RP Eye Research Foundation of Canada (R.R.M.), MRC of Canada (M.R.H. and B.R.L.), the Canadian Genetic Disease Network (R.R.M. and M.R.H.) and the Huntington Disease Society of America (M.R.H.). M.R.H. is an Established Investigator of the BC Children's Hospital. R.R.M. is an International Research Scholar of the Howard Hughes Medical Institute.

Correspondence and requests for materials should be addressed to R.R.M. (e-mail: mcinnes@sickkids.on.ca).

Genetic ablation of parathyroid glands reveals another source of parathyroid hormone

Thomas Günther*†, Zhou-Feng Chen†‡, Jaesang Kim§, Matthias Priemel‖, Johannes M. Rueger‖, Michael Amling‖, Jane M. Moseley¶, T. John Martin¶, David J. Anderson§ & Gerard Karsenty*

** Department of Molecular and Human Genetics, Program of Developmental Biology, Baylor College of Medicine, 1 Baylor Plaza, Houston, Texas 77030, USA*
‡ Department of Anesthesiology, Washington University School of Medicine, 660 South Euclid Avenue, St. Louis, Missouri 63110, USA
§ Howard Hughes Medical Institute and Division of Biology, California Institute of Technology, Pasadena, California 91125, USA
‖ Department of Trauma Surgery, Hamburg University, Martinistrasse 52, 20246 Hamburg, Germany
¶ St. Vincent's Institute of Medical Research, 9 Princes Street, Fitzroy 3065, Melbourne, Victoria, Australia
† These authors contributed equally to this work

The parathyroid glands are the only known source of circulating parathyroid hormone (PTH), which initiates an endocrine cascade that regulates serum calcium concentration[1]. *Glial cells missing2* (*Gcm2*), a mouse homologue of *Drosophila Gcm*, is the only transcription factor whose expression is restricted to the parathyroid glands[2–5]. Here we show that *Gcm2*-deficient mice lack parathyroid glands and exhibit a biological hypoparathyroidism, identifying *Gcm2* as a master regulatory gene of parathyroid gland development. Unlike *PTH receptor*-deficient mice, however, *Gcm2*-deficient mice are viable and fertile, and have only a mildly abnormal bone phenotype. Despite their lack of parathyroid glands, *Gcm2*-deficient mice have PTH serum levels identical to those of wild-type mice, as do parathyroidectomized wild-type animals. Expression and ablation studies identified the thymus, where *Gcm1*, another Gcm homologue, is expressed, as the additional, downregulatable source of PTH. Thus, *Gcm2* deletion uncovers an auxiliary mechanism for the regulation of calcium homeostasis in the absence of parathyroid glands. We propose that this backup mechanism may be a general feature of endocrine regulation.

Serum calcium is essential for many physiological functions including muscle contraction, blood coagulation, neuromuscular excitability and mineralization of bone, a tissue that contains 99%